THE ASTROPHYSICAL JOURNAL, 469:572–580, 1996 October 1

A SEARCH FOR ULTRAHIGH-ENERGY GAMMA RAYS FROM EGRET-DETECTED ACTIVE GALACTIC NUCLEI USING CASA-MIA

M. CATANESE,[1,2] A. BORIONE,[3] C. E. COVAULT,[3] J. W. CRONIN,[3] B. E. FICK,[3] L. F. FORTSON,[3] K. G. GIBBS,[3] M. A. K. GLASMACHER,[1] K. D. GREEN,[3] D. KIEDA,[4] J. MATTHEWS,[1] B. J. NEWPORT,[3] D. NITZ,[1] R. A. ONG,[3] D. SINCLAIR,[1] AND J. C. VAN DER VELDE[1]

Received 1995 November 20; accepted 1996 April 16

ABSTRACT

Extensive air shower data collected using the CASA-MIA detector are examined for evidence of gamma rays above 50 TeV from the directions of 32 active galactic nuclei. Gamma rays above 100 MeV from all of these objects have been detected previously by the Energetic Gamma Ray Experiment Telescope aboard the *Compton Gamma Ray Observatory*. One of these, Markarian 421, has also been observed by the Whipple Observatory Gamma Ray Telescope to emit TeV gamma rays. No evidence of continuous or short-term emission is found for data collected between 1990 March and 1994 November. The flux limits calculated from these data indicate a reduction in the signal extrapolated from the EGRET data, which is consistent with microwave attenuation of the gamma-ray spectra.

Subject headings: cosmic rays — galaxies: active — galaxies: nuclei — gamma rays: observations

1. INTRODUCTION

The sources of cosmic rays have remained a mystery since their discovery (Hess 1912). Their origins must be investigated indirectly because magnetic fields within the galaxy cause the tracks of the cosmic rays, except possibly those with energies above 10^{18} eV, to become unrelated to their source direction during their travel to Earth. Ultrahigh-energy gamma rays ($E \gtrsim 5 \times 10^{13}$ eV) could provide an indirect signal for sources of cosmic rays because they point back to their source and are difficult to produce except as the by-products of nuclear interactions. Searches for gamma rays at these energies have concentrated on galactic objects because lower energy gamma rays have been detected from objects like the Crab (Weekes et al. 1989; Baillon et al. 1993) and because there have been claims of ultrahigh-energy signals from Cygnus X-3 (Samorski & Stamm 1983) and Hercules X-1 (Dingus et al. 1988), among others. The observations of gamma rays with energies above 100 MeV from the directions of more than 40 active galactic nuclei (AGNs) (Fichtel et al. 1994; von Montigny et al. 1995) by the Energetic Gamma Ray Experiment Telescope (EGRET) aboard the *Compton Gamma Ray Observatory* suggest that extragalactic objects may also contribute to the cosmic-ray flux. Markarian 421, which is one of the AGNs seen by EGRET, has also been detected above 5×10^{11} eV (0.5 TeV) by the ground-based Whipple Observatory Gamma Ray Telescope (Punch et al. 1992).

The gamma rays from the AGNs have power-law spectra (i.e., $dN/dE \propto E^{-\gamma}$) with spectral indices, γ, between 1.4 and 2.6 in the EGRET energy range (von Montigny et al. 1995). If these spectra continue without change to ultrahigh energies, some of these AGNs would emit a gamma-ray flux of $\gtrsim 10^{-14}$ cm^{-2} s^{-1} above 10^{14} eV which would be detectable by air shower arrays like the Chicago Air Shower Array–Michigan Muon Array (CASA-MIA) experiment.

The search for emission from some of the objects in this work have been conducted before by other air shower arrays operating at similar energies to CASA-MIA (e.g., Alexandreas et al. 1993a; Amenomori et al. 1994), all with null results. However, as discussed in the following sections, this study uses a much larger data set and CASA-MIA has better background rejection because of its muon coverage. Also, this search covers a different time period than those covered in previous searches, which improves the coverage in the search for variable emission from these objects. So, this work extends the reach of the previous searches.

The mechanism which produces gamma rays in AGNs determines whether their power-law spectra can extend over the six orders of magnitude between the EGRET energy and that of CASA-MIA. This mechanism is currently unknown, though the emission seen by EGRET seems linked to the radio jets of some AGNs because EGRET has detected only AGNs in the *blazar* class (containing BL Lacertae objects, highly polarized ($>3\%$) quasars, and optically violent variable quasars) (Dermer & Schlickeiser 1992; Hartman et al. 1994). One popular model of AGNs posits that all AGNs are the same type of object and that the different classes of AGNs arise simply because they have different orientations relative to Earth. AGNs in the blazar class are believed to have jets very nearly aligned along our line of sight. It has been proposed (Dermer & Schlickeiser 1992) that the gamma rays from the AGNs seen by EGRET result from inverse Compton scattering of low-energy photons by energetic electrons inside the jets. If this model is correct, it is unlikely that the AGNs generate ultrahigh-energy gamma rays through the same mechanism because synchrotron losses make it difficult to accelerate enough electrons to the energies required for producing a detectable flux of ultrahigh-energy gamma rays. However, as pointed out by von Montigny et al. (1995), inverse Compton models have difficulty explaining even the TeV emission from Markarian 421 seen by Whipple.

Models in which gamma rays are the end products of the interactions of nuclei rather than leptons bypass many of these difficulties and leave open the possibility that gamma rays with energies above 50 TeV may be produced. In all of these models, the nuclei are accelerated via first-order

[1] Department of Physics, University of Michigan, Ann Arbor, MI 48109.
[2] Postal address: Whipple Observatory, P.O. Box 97, Amado, AZ 85645.
[3] Enrico Fermi Institute, University of Chicago, Chicago, IL 60637.
[4] Department of Physics, University of Utah, Salt Lake City, UT 84112.

Fermi shock accelaration. Nuclei are very unlikely to escape the acceleration region because of the magnetic fields there, but they produce neutrons, which can escape if the matter density in the acceleration region is not too high. The neutrons eventually decay ($n \rightarrow pe^{-}\bar{\nu}_e$) and the protons and electrons contribute gamma rays through secondary interactions. Gamma rays that result from neutral pions are not expected to escape the high radiation density near the AGNs. In the model of Biermann et al., the nuclei are accelerated upon encountering shocks within the jets (Biermann & Strittmatter 1987) and also within the "hot spots" at the end of the AGN's jets (Rachen & Biermann 1993). This mechanism would contribute cosmic-ray protons above 10^{18} eV (Rachen, Stanev, & Biermann 1993). By contrast, in the model of Szabo & Protheroe (1992) the nuclei are accelerated in a shock which forms in an accretion disk near the AGNs and the resultant, unbeamed protons have energies between 10^{15} and 10^{17} eV.

Even if ultrahigh-energy gamma rays are produced, they may not survive the long trip from the AGNs to Earth. As was shown almost 30 yr ago (Gould & Schréder 1967), the distance which gamma rays can travel is limited by photon-photon interactions with low-energy background radiation fields: $\gamma + \gamma \rightarrow e^{-} + e^{+}$. Gamma rays which scatter on intergalactic photons are lost from the spectrum that reaches Earth because even very weak intergalactic magnetic fields (e.g., $B \sim 10^{-10}$ G) change the directions of the electrons and positrons enough so that only a small fraction of the gamma rays produced by their interactions point back to their source (Protheroe 1986). For gamma rays above 50 TeV, the cosmic microwave background radiation (CMBR) and intergalactic infrared radiation fields (IIRF) are the most important interaction fields. The CMBR spectrum is well known (Mather et al. 1994) and produces a cutoff in the gamma-ray spectra above an energy which varies with the redshift of the source. For a relatively nearby AGN like Markarian 421 ($z = 0.031$) the CMBR interaction would eliminate gamma rays with energies above 10^{14} eV and for a more distant AGN like $1633+382$ ($z = 1.81$) the cutoff would occur at 10^{13} eV. We have treated the absorption of gamma rays on the CMBR in detail; the calculation is described in § 5 below.

In contrast to the CMBR, attempts to measure the density of the IIRF directly (Kawada et al. 1994; Dube, Wickes, & Wilkinson 1979) have provided only upper limits which are well above theoretical expectations. Theoretical estimates of the IIRF density (e.g., Stecker, de Jager, & Salamon 1992; Tyson 1990; MacMinn & Primack 1995) can be used to illustrate the possible effects of the IIRF on gamma rays. If the IIRF does lie within the range of these models, interaction with the IR photons would cut off the AGNs gamma-ray spectra in the TeV energy range, thereby eliminating all the gamma rays to which CASA-MIA would be sensitive. However, observations of Markarian 421 with the Whipple Observatory Gamma Ray Telescope show no significant absorption features up to 3 TeV (Mohanty et al. 1993) whereas the model of Stecker et al. (1992) indicates that a cutoff would occur at a lower energy than this. Due to this uncertainty, we do not consider IR absorption of gamma rays in the following analysis, although it could be significant.

A detection of ultrahigh-energy emission from sources also observed by either Whipple or EGRET would place strong constraints on the emission mechanism at all gamma-ray wavelengths. Also, the detection of ultrahigh-energy emission from *any* extragalactic sources would constrain the density of the background IIRF to a level well below theoretical expectations. Finally, we note that the standard cosmology with a universal CMBR and cosmological distance scale to AGNs implies that no gamma-ray emission is expected above the microwave cutoff ($\gtrsim 100$ TeV). In the unlikely event that *any* extragalactic source was detected above this cutoff it would be very difficult to explain under standard model cosmologies. So, while our main goal is to attempt to observe gamma rays near the CMBR cutoff point, it is worthwhile to look beyond this point as well.

2. THE CASA-MIA INSTRUMENT

The CASA-MIA detector (Fig. 1) is located in Dugway, Utah (40°.2 N, 112°.8 W) at a mean atmospheric depth of 870 g cm^{-2}. CASA (Borione et al. 1994a) and MIA (Sinclair 1989) have been described in detail elsewhere. CASA is a surface scintillator array consisting of 1089 detector stations with an enclosed area of 2.3×10^5 m^2. A detector station consists of four plastic scintillators, each viewed by a phototube, with associated electronics and power supplies. To reduce the effects of counter noise and accidental hits from air showers below CASA-MIA's threshold, only "alerted" CASA stations, those with two or more counters which detect the passage of particles within 30 ns of each other, record data. MIA consists of 1024 buried scintillators grouped into 16 patches of 64 counters. Its total active area, 2500 m^2, provides 10 times the muon coverage of any other air shower array in existence, permitting excellent hadron rejection. The detector's combination of collection area and muon coverage makes it sensitive to a very low flux of gamma rays in its energy range.

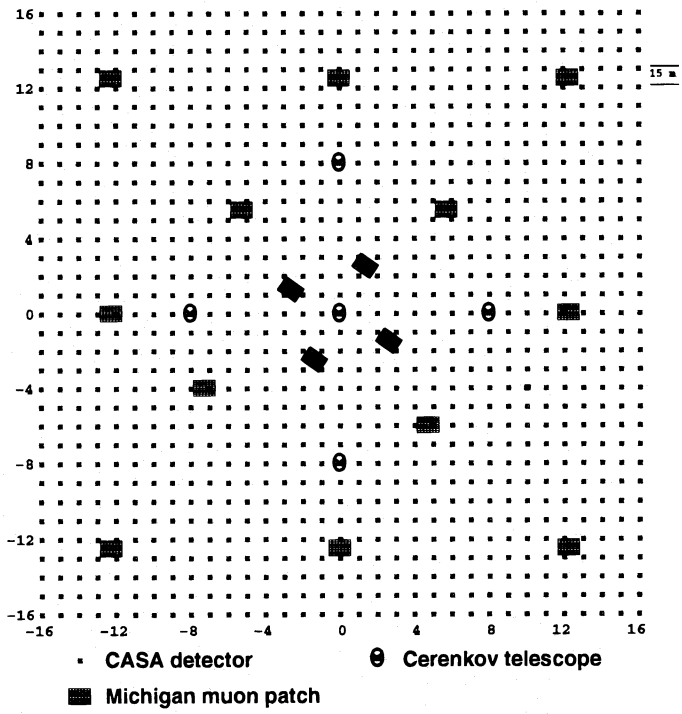

FIG. 1.—Schematic diagram of the CASA-MIA experiment. The main components used to collect data are the CASA detector stations (*small black squares*) and the MIA muon patches (*hatched rectangles*). The Cerenkov telescopes (*crossed ovals*) are used for angular resolution studies.

Data are collected in runs typically lasting 6 hr. A triggered event is one in which at least three CASA detector stations record particles in three or more counters within 10 μs. The average trigger rate is about 20 events s^{-1} and the duty factor is better than 0.90. Shower cores, directions, and sizes are calculated off-line. Shower sizes consist of the number of muons, or muon size, (N_μ) and the number of positrons and electrons, or electron size, (N_e) in the event. The muon size is determined using a maximum likelihood fit which compares the distribution of hit and unhit muon counters, minus the effects of counter noise, to a standard lateral distribution function (Greisen 1960)

$$\rho_\mu(r) = N_\mu k_\mu \left(\frac{r}{r_0}\right)^{-0.75} \left(1 + \frac{r}{r_0}\right)^{-2.5}, \quad (1)$$

where k_μ is the normalization constant for the muons, r is the distance to the shower core, and $r_0 = 300$ m. The electron size is determined by a maximum likelihood fit which compares the distribution of detected particles, minus the contributions of counter noise and the muons, to the Nishimura-Kamata-Greisen lateral distribution function (Greisen 1960)

$$\rho_e(r) = \frac{N_e}{r_1^2} \left(\frac{r}{r_1}\right)^{s-2} \left(1 + \frac{r}{r_1}\right)^{s-4.5} \frac{\Gamma(4.5 - s)}{2\pi\Gamma(s)\Gamma(4.5 - 2s)}, \quad (2)$$

where s is the shower age and $r_1 = 80$ m gives the best fit to the data. An average shower has 19 alerted stations, an electron size of $10^{4.5}$, and a muon size of $10^{3.4}$.

The data used in this search were collected between 1990 March and 1994 November with a gap from 1991 April to 1991 December to repair damage caused by lightning. During this time, CASA-MIA detected more than 2×10^9 events. After data processing and quality cuts, the total number of events is 1.35×10^9, of which 1.20×10^9 have valid muon information which is the largest data set used in a search for gamma rays from AGNs by an air shower array.

3. BACKGROUND REJECTION

The vast majority of events detected by air shower arrays are initiated by cosmic rays. In order to detect a gamma-ray signal, we must reduce this background. Because the cosmic rays are isotropic and gamma rays from a point source are tightly centered on the source direction, the array's angular resolution determines a bin size for collecting on-source data which optimizes the signal (gamma rays) to noise (cosmic rays) ratio. Also, an air shower initiated by a cosmic ray is expected to have $\sim$30 times as many muons as a shower of the same size initiated by a gamma ray (Stanev, Gaisser, & Halzen 1985), so we can improve CASA-MIA's sensitivity to gamma rays by selecting events with muon sizes which are small relative to what is expected for showers initiated by cosmic rays.

The angular resolution of CASA has been determined by observation of the shadow of the Moon (Borione et al. 1994b), by coincident detection of events with the Utah Cherenkov Telescope Array (Elbert et al. 1990), and by the divided array method (Borione et al. 1994a). We express the angular resolution of CASA in terms of σ_{63}, the half-angle of a circular bin which contains 63% of the photons from a point source. The standard deviation, σ, of a symmetric two-dimensional Gaussian distribution, a figure often used for quoting an array's angular precision, is equal to $\sigma_{63}/\sqrt{2}$. The optimum circular bin for a point source has half-angle $1.12\ \sigma_{63} = 1.59\ \sigma$. Such a bin contains 72% of the signal from a point source. CASA's angular resolution improves from $\sigma_{63} = 1.^\circ 8$ for showers with less than 16,000 particles to $\sigma_{63} = 0.^\circ 5$ for showers with more than 100,000 particles. We have found that the angular resolution scales more closely with the number of alerted CASA stations than with the fitted electron size. Therefore, we parameterize the optimum bin size in terms of the number of alerted stations. The optimum size for a collection bin decreases from a half-angle of $2.^\circ 46$ for events with 10 or fewer alerted stations to $0.^\circ 39$ for events with more than 60 alerted stations.

We characterize the muon content of a shower by the variable $R_\mu = \log_{10} N_\mu - \langle \log_{10} N_\mu \rangle$, where N_μ is the shower's muon size and $\langle \log_{10} N_\mu \rangle$ is the mean base-10 logarithm of the muon size for the shower. The quantity $\langle \log_{10} N_\mu \rangle$ is well represented by the function

$$\langle \log_{10} N_\mu \rangle = a + b \sec\theta + c \log_{10} N_t + d \sec\theta \log_{10} N_t, \quad (3)$$

where $N_t = N_e + N_\mu$ is the shower's "total" size and θ is the shower zenith angle. Using N_t instead of N_e improves the fit to the coefficients (a, b, c, d) which improves the hadron rejection. The coefficients are determined individually for each run in the data because they depend on atmospheric conditions and the status of the arrays. Simulations (Catanese 1994) indicate that the best signal-to-noise ratio is obtained by identifying all events with $R_\mu < -1$ as gamma-ray candidates. This cut eliminates 90% of the cosmic-ray background for all data while retaining about 75% of the gamma rays.

4. SEARCH METHOD

Candidate source events are those having directions which fall within a circular bin centered on the position of an AGN. The bin's angular size is specified by the number of alerted stations in the event. In this way, the bin size is optimized for each shower and we avoid the reduction in sensitivity which would occur at the largest and smallest sizes if a fixed bin were used. Muon poor events ($R_\mu < -1$) are considered gamma-ray candidates. We also divide the data into two shower size databases, those with less than $10^{4.4}$ electrons and those with greater than $10^{4.4}$ electrons. Gamma rays which survive the CMBR interaction between the AGN and Earth are expected to be of lower energy so they should produce only small air showers. Thus, the $N_e < 10^{4.4}$ grouping may improve CASA-MIA's sensitivity to the AGN's emission. This cut is not optimum because the energy associated with showers of a given size increases rapidly with increasing zenith angle. The $N_e > 10^{4.4}$ size bin would actually provide greater sensitivity to the gamma rays if their spectra continue unchanged from EGRET to CASA-MIA energies. This is because the EGRET spectra are harder than the cosmic-ray spectrum (so the gamma rays would make up a larger percentage of the on-source data) and because the CASA-MIA background rejection improves with increasing shower size.

We calculate the cosmic-ray background contribution to the on-source data as follows. All events within a declination (δ) band centered on the source declination are collected for each run. These events' local times are replaced with the local times of 20 other events in the collection while the original events' positions in local coordinates are main-

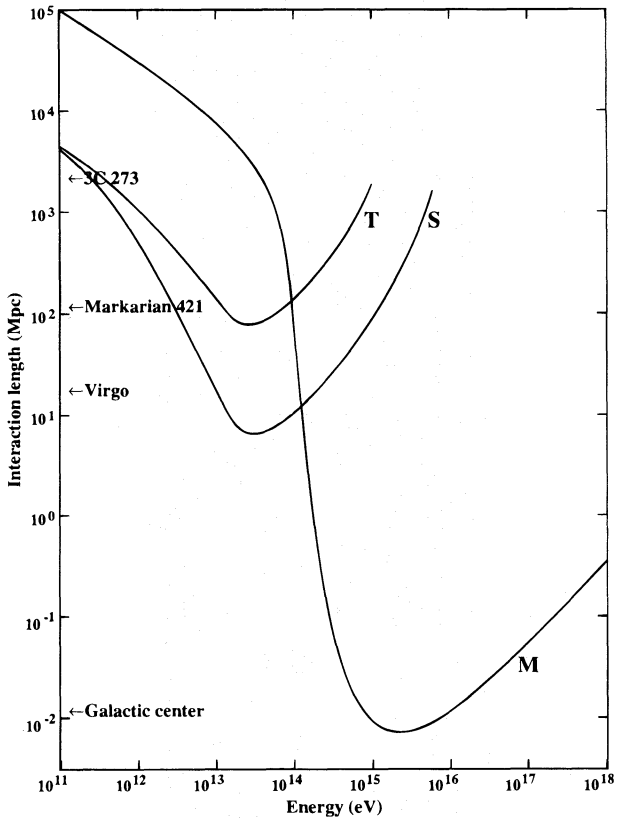

FIG. 2.—Photon-photon pair production interaction lengths vs. energy for the CMBR (M) and the IIRF. The IIRF estimate of Stecker et al. (1992) is used to give the interaction curve indicated by the "S" and the curve labeled with the "T" is derived from the IIRF estimate of Tyson (1990). The interaction lengths account for changes in the gamma rays and background fields with the aging of the universe.

tained. This gives each event 20 new right ascensions (α's). If a new α places an event within a point source search bin centered on the source direction, it is a background event. Each background event is assigned a weight of 1/20 to account for the added effective exposure. This method is quite similar to those described by Alexandreas et al. (1993b) and Cassiday et al. (1989).

Many of the EGRET sources show variability in their emission (Kniffen et al. 1993; Mattox et al. 1993) and Markarian 421 has shown variability at very high energies (VHEs) (Kerrick et al. 1995a, 1995b; Schubnell et al. 1995), though not at EGRET energies (Lin et al. 1993). So, in addition to searching for continuous emission in the whole data set, we look for emission on individual days, weeks, and months.

5. FROM COLLECTED DATA TO SOURCE FLUX

The significance of an excess or deficit in the on-source data relative to the estimated background is determined using the prescription of Li & Ma (1983). A significant excess is interpreted as a signal and the number of gamma rays, N_γ, is estimated. If no signal is seen, a 90% confidence upper limit, N_γ^{90}, is calculated using the method of Helene (1983). The ratio of N_γ, or N_γ^{90}, to the number of background events in the all-muon data set, $B_{\rm all}$, is f_γ, or f_γ^{90}, which is one estimate of the fraction, or upper limit on the fraction, of the cosmic-ray flux which is gamma rays. For the remainder of this section we use N_γ^{90} and f_γ^{90} in discussing the calculation of gamma-ray flux limits. N_γ and f_γ can be substituted for N_γ^{90} and f_γ^{90}, respectively, and in that case the phrase "flux limit" should be replaced by the word "flux."

TABLE 1

EGRET AGNs VISIBLE TO CASA-MIA[a]

AGN ID	AGN Name	α (hrs.)	δ (°)	z	Integral flux[b]	Differential spectral index[c]
(1)	0202+149	2.07	15.2	···	0.25±0.08	2.4±0.2
(2)	0234+285	2.62	28.8	1.213	0.17±0.05	2.4±0.3
(3)	0235+164	2.64	16.6	0.94	0.86±0.12	2.0±0.2
(4)	0420-014	4.38	-1.4	0.92	0.50±0.14	1.9±0.3
(5)	0446+112	4.81	11.3	···	0.96±0.18	1.8±0.3
(6)	0458-020	5.01	-2.0	2.286	0.62±0.15	···
(7)	0528+134	5.51	13.5	2.06	0.84±0.10	2.6±0.1
(8)	0716+714	7.35	71.4	···	0.18±0.04	2.0±0.3
(9)	0804+499	8.13	49.9	1.43	0.21±0.08	2.5±0.2
(10)	0827+243	8.51	24.2	2.046	0.21	2.2±0.4
(11)	0829+046	8.52	4.4	0.18	0.14±0.05	···
(12)	0836+710	8.68	70.9	2.17	0.13±0.03	2.4±0.2
(13)	0954+658	9.97	65.6	0.368	0.21	1.7±0.2
(14)	Mrk 421	11.07	38.5	0.031	0.14±0.05	1.7±0.2
(15)	1156+295	11.99	29.3	0.729	0.63	1.8±0.4
(16)	1219+285	12.35	28.3	0.102	0.17	1.4±0.4
(17)	1222+216	12.41	21.4	0.435	0.17	2.4±0.2
(18)	3C 273	12.48	2.1	0.158	0.26±0.04	2.4±0.1
(19)	1229-021	12.53	-2.4	1.045	0.12±0.03	···
(20)	3C 279	12.93	-5.8	0.538	0.85±0.07	2.1±0.1
(21)	1406-076	14.14	-7.8	1.494	1.01	1.9±0.1
(22)	1510-089	15.21	-9.1	0.361	0.17±0.07	2.6±0.4
(23)	1604+159	16.11	15.9	···	0.17±0.04	···
(24)	1606+106	16.14	10.5	1.23	0.53±0.12	2.2±0.3
(25)	1611+343	16.22	34.2	1.401	0.33	···
(26)	1633+382	16.58	38.2	1.81	0.95±0.08	1.9±0.1
(27)	1741-038	17.73	-3.8	1.054	0.34±0.09	3.0±0.4
(28)	2022-077	20.42	-7.6	···	0.67±0.12	1.5±0.2
(29)	2209+236	22.20	23.9	···	0.15±0.04	···
(30)	2230+114	22.54	11.7	1.037	0.25±0.05	2.6±0.2
(31)	2251+158	22.89	16.1	0.859	0.78±0.08	2.2±0.1
(32)	2356+196	23.97	19.9	1.066	0.29±0.09	···

[a] AGN list and flux values are from Fichtel et al. 1994 with the exceptions of AGNs (13), (15), (16), (17), and (25), which are from von Montigny et al. 1995.

[b] Flux estimates are in units of 10^{-6} cm^{-2} s^{-1} for $E > 100$ MeV.

[c] Spectral indices are from von Montigny et al. 1995.

To estimate the flux of gamma rays which would produce the measured f_γ^{90} we use a simulation program (Catanese 1994) which accurately models air showers and the response of CASA-MIA to them. We assume the gamma rays follow a single power-law spectrum from the EGRET energy to that of CASA-MIA with a point in the spectrum fixed at the EGRET flux for the AGNs. The background cosmic rays are simulated with the measured spectrum (Nagano et al. 1984) and composition (Muller et al. 1991). We vary the gamma-ray spectral index until we match the value of f_γ^{90} found in the data. This spectral index limit can be compared to the EGRET data and, in the case of Markarian 421, to the Whipple data as well.

A more common method of calculating a flux limit for air shower arrays (see, e.g., McKay et al. 1993; Alexandreas et al. 1993a) is to multiply f_γ^{90} by the cosmic-ray flux, with some correction factors to account for such things as the efficiency for gamma-ray detection. The flux limits are then quoted at the median energy for cosmic rays or gamma rays, depending on the particular application of the method.

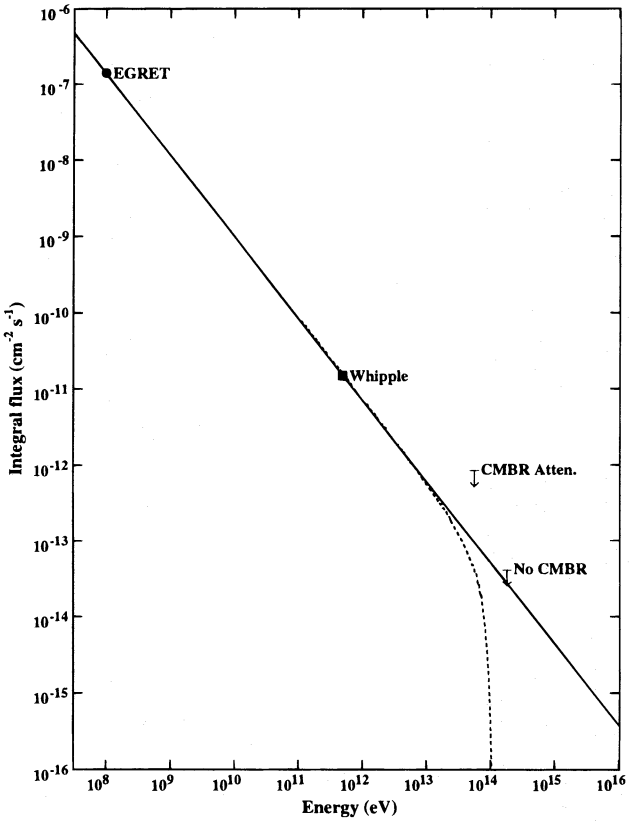

FIG. 3.—Markarian 421 flux limits for continuous emission. The EGRET (*circle*) (Fichtel et al. 1994) and Whipple (*square*) (Punch et al. 1992) flux points are shown. The solid line is an unattenuated spectrum which passes through the EGRET and Whipple points. The dashed line shows the spectrum after interaction with the CMBR has been included. The flux limits which ignore and include attenuation of the gamma-ray signal by the CMBR are shown.

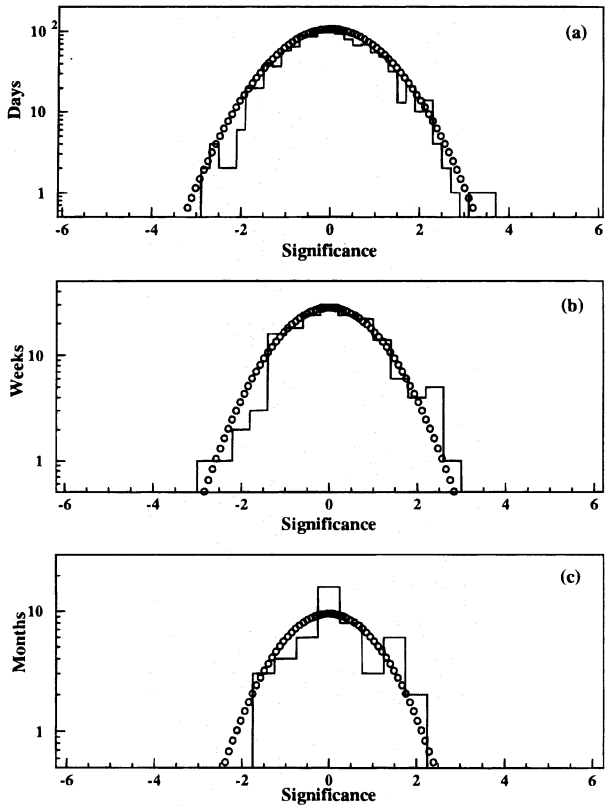

FIG. 4.—The distributions of significances for (*a*) daily, (*b*) weekly, and (*c*) monthly emission for Markarian 421. The circles show the expected distribution for Gaussian fluctuations of the cosmic-ray background.

If the spectrum used to calculate the median energy for this method is much steeper (e.g., McKay et al. 1993) than what is typically obtained with the method we use here (see Table 2), the median energies are much lower. The flux limits are also lower than those obtained with our method, regardless of the gamma-ray spectrum used. Because the flux limits calculated with different methods produce such very different results, the only model-independent comparison of flux limits for air shower arrays which can be made is to compare the upper limits on the fraction of the cosmic-ray flux in the data set, f_γ^{90} in this work. We decided to use our method because it incorporates factors like the efficiency for detecting gamma rays and cosmic rays in the simulation program so they are not applied as a single multiplicative constant. This also makes it easier to include the effects of the CMBR attenuation (see below). Finally, our method directly incorporates the EGRET and Whipple results, which are the most relevant reference points for these sources spectra, into the flux limit calculation.

Even if the AGNs produce a gamma-ray spectrum which follows a simple power-law from EGRET to CASA-MIA energies, the spectrum at Earth will not, because of the interaction between the gamma rays and the CMBR. To account for this effect in flux calculations, each simulated gamma ray is assigned a weight which equals the probability that it survives the trip from the AGN to Earth. If we do not wish to include the effect of CMBR attenuation in the flux limit, this weight is simply 1.0 for each gamma ray regardless of its energy or the AGN's distance.

For flux limit calculations which do include the CMBR interaction, the weight is determined in the following way. The probability that a gamma ray with energy E from a source at redshift z_0 reaches Earth without interacting with a CMBR photon is

$$P_{\text{arrival}} = e^{-\tau}, \tag{4}$$

where τ is the absorption "optical depth," given by

$$\tau(E, z_0) = \int_0^{z_0} dz \frac{dl}{dz} \frac{d\tau}{dl}, \tag{5}$$

and l is the distance from Earth to the source. The expression for $d\tau/dl$ at $z = 0$ is given by

$$\frac{d\tau}{dl}(E, z = 0) = \int_0^{\pi} \frac{1}{2}(1 - \cos\theta) \sin\theta \, d\theta \times \int_{[2m^2c^4/E(1-\cos\theta)]}^{\infty} d\epsilon \sigma(E, \epsilon, \theta) n(\epsilon) \tag{6}$$

(Gould & Schréder 1967). Here, θ is the angle between the gamma ray and the CMBR photon, ϵ is the CMBR photon energy, and σ is the cross section for photon-photon pair production. The lower limit on the integral over ϵ arises because pair production cannot occur if $\frac{1}{2}(1 - \cos\theta)E\epsilon < m^2c^4$. The density of the CMBR photons in units of cm^{-3} eV^{-1}, $n(\epsilon)$, is given by a blackbody spectrum,

$$n(\epsilon) = \frac{1}{(\hbar c)^3} \left(\frac{\epsilon}{\pi}\right)^2 \frac{1}{e^{\epsilon/kT} - 1} \tag{7}$$

with $T = 2.726$ K (Mather et al. 1994).

TABLE 2

CONTINUOUS EMISSION SEARCH RESULTS[a]

AGN	N_{on}	B	σ	f_γ^{90} $\times 10^{-3}$	No CMBR			CMBR Incl.		
					γ	E	I	γ	E	I
(1)	41328	41103	1.1	1.2	2.05	370	3.4	...	...	...
(2)	92502	92446	0.2	0.60	2.06	210	3.2	1.27	14	7.1×10^{5}
(3)	45752	45989	-1.1	0.50	2.19	300	1.7	...	...	...
(4)	5109	5216	-1.4	1.2	2.10	1800	0.49	...	...	...
(5)	28336	28324	0.1	0.94	2.15	440	2.3	...	...	...
(6)	4577	4640	-0.9	1.5	2.10	2000	0.56	...	...	...
(7)	34985	34872	0.6	1.0	2.14	380	2.8	...	...	...
(8)	38992	39242	-1.2	0.48	2.10	570	0.67	...	...	...
(9)	111564	111894	-1.0	0.35	2.12	190	2.0	...	...	...
(10)	73674	73766	-0.3	0.53	2.09	230	2.5	...	...	...
(11)	12258	12224	0.3	1.5	1.95	1000	3.1	...	...	...
(12)	40538	40738	-1.0	0.53	2.07	580	0.76	...	...	...
(13)	59809	60035	-0.9	0.43	2.10	370	1.3	1.62	38	7.3×10^{3}
(14)	117452	117119	0.9	0.69	2.04	180	4.3	1.90	56	8.8×10^{1}
(15)	94978	95070	-0.3	0.47	2.18	180	2.8	1.77	22	4.9×10^{3}
(16)	92082	91954	0.4	0.61	2.06	210	3.2	1.88	50	1.7×10^{2}
(17)	64737	65023	-1.1	0.42	2.09	260	1.8	1.68	33	2.8×10^{3}
(18)	9096	9182	-0.9	1.1	2.06	1200	0.78	...	...	...
(19)	4455	4493	-0.5	1.8	1.92	2600	1.7	...	...	...
(20)	2421	2402	0.4	3.5	2.07	3600	0.68	...	...	...
(21)	1594	1574	0.5	4.6	2.06	5000	0.72	...	...	...
(22)	1190	1184	0.2	4.6	1.96	7100	0.48	...	...	...
(23)	44667	44470	0.9	1.0	2.03	370	3.0	...	...	...
(24)	26961	26868	0.6	1.1	2.10	500	2.4	...	...	...
(25)	112411	112253	0.5	0.58	2.12	170	3.5	...	...	...
(26)	120342	120751	-1.1	0.32	2.25	140	1.8	...	...	...
(27)	3517	3507	0.2	2.6	2.03	2700	0.71	...	...	...
(28)	1642	1665	-0.6	3.1	2.06	4900	0.45	...	...	...
(29)	76939	76664	1.0	0.85	2.03	240	3.8	...	...	...
(30)	30657	30643	0.1	0.90	2.06	480	2.0	...	...	...
(31)	45916	45671	1.1	1.1	2.13	320	3.6	1.38	21	7.5×10^{5}
(32)	60102	59723	1.5	1.1	2.06	280	4.2	1.33	17	5.1×10^{5}

[a] In this table, N_{on} is the number of on-source events, B is the estimated background, σ is the significance of the excess or deficit of N_{on} relative to B, f_γ^{90} is defined in the text, I is the integral flux limit in units of 10^{-14} cm^{-2} s^{-1}, γ is the differential spectral index limit, and E is the median energy of the gamma rays in TeV for a power-law spectrum with index γ. The columns under the heading "No CMBR" do not include the effects of the interaction between the gamma rays and the CMBR, while those entries under the heading "CMBR Incl." do include those effects.

Due to the large distances to the AGN, using $d\tau/dl$ at $z = 0$ is not sufficient for properly calculating τ. A gamma ray which had an energy $E(1 + z)$ when it was emitted from an AGN at a redshift of z will have an energy E at Earth due to expansion of the universe. At the time of emission, the blackbody photons would have had a higher density and higher mean energy than at present. This is equivalent to replacing T with $T(1 + z)$ in equation (7), where T is the present temperature of the CMBR. To calculate τ for an AGN, we replace E by $E(1 + z)$ and T by $T(1 + z)$ for the variables in equations (6) and (7) before integrating over z. We assume a Friedmann-Robertson-Walker cosmology,

$$\frac{dl}{dz} = \frac{c}{H_0}\frac{1}{(1+z)^2(1+\Omega z)^{1/2}},$$

so that if we set $\Omega = 1$, we obtain

$$\tau(E, z_0) = \frac{c}{H_0}\int_0^{z_0} dz(1+z)^{1/2}\int_0^2 dx\,\frac{x}{2} \times \int_{[2m^2c^4/Ex(1+z)^2]}^{\infty} d\epsilon' n(\epsilon')\sigma[E(1+z), \epsilon'(1+z), x] \quad (8)$$

(Stecker 1971). Here $x = (1 - \cos\theta)$, $\epsilon' = \epsilon/(1 + z)$, and $H_0 \approx 75$ km s^{-1} Mpc^{-1} is the assumed Hubble constant. The distance at which $\tau = 1$ is a measure of how far a gamma ray can travel without interacting with the CMBR. Figure 2, which is obtained by numerically integrating equation (8), shows this interaction length as a function of gamma-ray energy. The distances to some relevant celestial objects are shown for reference. The effect of the redshift corrections becomes important for AGNs more distant than 1000 Mpc.

Also included in Figure 2 are interaction length curves where the CMBR $n(\epsilon)$ has been replaced by two of the model background IIRF densities cited in § 1. The "S" indicates the mean free path for gamma rays traveling through the IIRF field described by Stecker et al. (1992) and the "T" is derived from the IIRF estimate of Tyson (1990). These curves show that the IR interaction may dominate the effects of the CMBR for all gamma rays below $\sim 10^{14}$ eV.

6. RESULTS AND DISCUSSION

We have searched for continuous and episodic emission of ultrahigh-energy gamma rays from the directions of 32 AGNs which pass within the CASA-MIA field of view. The

AGNs, their positions in right ascension and declination, their redshifts, and the flux above 100 MeV and differential spectral energy index measured by EGRET are shown in Table 1. A blank entry in the table indicates that the quantity is unknown. Markarian 421 is the most likely candidate to emit gamma rays which are detectable by CASA-MIA because it is the closest of the EGRET AGN to Earth, it transits near the Dugway zenith (so the CASA-MIA energy threshold for this object is low), and it has been detected at TeV energies.

Table 2 contains the results of the search for continuous gamma-ray emission. For brevity, we show only the muon poor ($R_\mu < -1$) subset of the all-data sample (no size cuts) but the results for the other data sets lead to the same conclusion. We see no evidence of continuous ultrahigh-energy emission for any of the sources in the EGRET list which are visible to CASA-MIA. The largest excess, that of AGN (32) (2356+196), is consistent with statistical fluctuations of the background in the on-source region. Note that flux limits which include the interaction with the CMBR are not calculated for most of the AGNs. Those AGNs have transits which are so low in the sky or they are so distant that CASA-MIA is not sensitive to air showers produced by gamma rays below their CMBR cutoff. Also, if an AGN's redshift is unknown, a flux limit which includes CMBR attenuation cannot be calculated.

A spectral index limit which is larger than the EGRET spectral index indicates that the gamma-ray flux at CASA-MIA's energies is lower than what is expected from an extrapolation of the EGRET flux along the spectrum measured at EGRET's energies. For the limits which do not include the attenuation from the CMBR, this may be the result of the CMBR interaction or a decrease in the emission at the source. For a flux limit which does include the

TABLE 3

TRANSIENT EMISSION SEARCH RESULTS[a]

AGN	Daily σ	Daily γ	Daily E	Daily I	Weekly σ	Weekly γ	Weekly E	Weekly I	Monthly σ	Monthly γ	Monthly E	Monthly I
No CMBR attenuation												
(1)	3.2	1.71	640	38	2.1	1.87	480	4.0	2.2	1.91	450	2.1
(2)	2.9	1.77	330	17	3.5	1.83	300	7.1	2.1	1.90	260	3.0
(3)	3.2	1.85	450	18	2.7	1.94	400	5.5	1.7	1.95	390	4.8
(4)	2.9	1.78	2800	7.9	2.4	1.88	2400	1.6	1.9	1.87	2430	1.9
(5)	2.7	1.86	640	13	2.2	1.94	560	4.3	3.3	1.95	560	3.5
(6)	2.9	1.82	2800	4.6	3.4	1.86	2600	2.5	1.8	1.94	2400	0.69
(7)	2.7	1.85	550	15	2.8	1.93	500	5.2	2.9	1.97	470	2.9
(8)	3.2	1.66	1200	36	2.0	1.87	780	1.8	1.6	1.91	730	0.97
(9)	3.2	1.78	310	18	1.9	1.87	260	5.2	1.3	1.95	230	1.9
(10)	2.8	1.78	350	16	2.8	1.85	310	6.2	2.4	1.89	300	3.4
(11)	3.1	1.72	1500	8.7	2.6	1.81	1300	2.3	1.9	1.86	1200	1.2
(12)	2.8	1.74	970	9.2	1.7	1.85	790	1.7	1.9	1.89	750	1.0
(13)	2.7	1.73	660	21	1.8	1.88	500	2.7	2.0	1.90	490	2.0
(14)	3.6	1.73	310	27	2.9	1.86	240	4.9	1.8	1.91	220	2.3
(15)	3.3	1.86	270	19	2.2	1.93	240	7.0	1.5	2.00	220	2.8
(16)	3.7	1.76	330	20	2.6	1.85	280	6.0	1.7	1.92	260	2.3
(17)	2.9	1.76	430	16	2.4	1.84	360	5.5	1.4	1.95	310	1.2
(18)	3.6	1.70	2200	20	3.0	1.76	1900	7.5	1.7	1.88	1500	1.2
(19)	3.2	1.61	4300	26	3.0	1.70	3600	5.8	2.0	1.74	3300	3.2
(20)	3.0	1.78	5000	8.5	2.3	1.89	4400	1.4	2.0	1.94	4000	0.57
(21)	4.1	1.91	5900	8.3	2.3	2.01	5300	1.5	2.9	2.05	5000	0.76
(22)	2.9	1.67	9800	7.7	2.3	1.78	8600	1.1	1.8	1.83	8100	0.45
(23)	3.4	1.77	550	12	2.7	1.81	520	6.2	2.0	1.90	440	1.9
(24)	2.9	1.80	750	17	3.0	1.89	640	4.8	2.2	1.93	600	2.5
(25)	3.3	1.81	270	19	2.0	1.90	230	6.3	1.3	1.91	230	5.1
(26)	3.4	1.90	220	18	2.4	1.98	200	6.1	1.7	2.05	180	2.7
(27)	3.7	1.74	4000	7.6	2.3	1.85	3400	1.4	2.5	1.89	3200	0.76
(28)	2.8	1.77	6900	5.6	2.6	1.85	6300	1.6	2.3	1.87	6200	1.2
(29)	2.9	1.76	380	16	2.7	1.84	320	5.4	2.2	1.88	300	2.8
(30)	2.8	1.76	740	15	2.3	1.81	700	7.4	2.4	1.91	600	1.8
(31)	3.0	1.85	460	18	1.9	1.95	390	4.3	2.5	1.98	380	2.7
(32)	3.6	1.78	430	18	3.3	1.86	380	6.0	3.0	1.86	380	6.8
CMBR attenuation included												
(13)	...	...	...	...	1.8	1.32	38	3.3×10^4	2.0	1.36	38	2.2×10^4
(14)	3.6	1.54	59	1.1×10^3	2.9	1.69	58	1.4×10^2	1.8	1.76	57	6.2×10^1
(15)	3.3	1.35	22	8.2×10^4	2.2	1.46	22	2.3×10^4	1.5	1.55	22	7.3×10^3
(16)	3.7	1.51	52	2.1×10^3	2.6	1.62	51	5.0×10^2	1.7	1.70	51	1.7×10^2
(17)	2.9	1.23	33	9.7×10^4	2.4	1.35	33	1.9×10^4	1.4	1.50	33	3.0×10^3

[a] In this table, σ is the maximum significance for any day, week, and month in the data set for the AGNs, γ is the spectral index limit, E is the median energy of the gamma rays in TeV for a power-law spectrum with index γ, and I is the integral flux limit in units of 10^{-13} cm^{-2} s^{-1}. The section of the table headed by the phrase "No CMBR attenuation" contains flux and spectral index limits which are calculated without including the effects of the interaction between the gamma rays and CMBR. The section of the table headed by the phrase "CMBR attenuation included" contains flux and spectral index limits which do include the effects of the interaction between the gamma rays and the CMBR.

effects of the CMBR interaction, a larger spectral index limit would indicate that the flux at CASA-MIA's energy is lower than can be accounted for with CMBR interactions alone. Attenuation by IR photons or a change in the spectrum at the source would cause such a decrease. The limits from our data on the spectral indices for AGN (3), (4), (5), (8), (12), (13), (15), (16), (21), (26), and (28) are lower than the EGRET measurements if the CMBR interaction is not included. Of these, AGN (5), (16), (21), (26), and (28) are outside the EGRET spectral index range. Only AGN (16), 1219+285, has a flux limit which includes CMBR interactions that is below the EGRET expectation. Its spectral index limit lies outside the EGRET range, providing a clear indication that the gamma-ray flux is lower at CASA-MIA's energies than can be accounted for by CMBR interaction alone.

As discussed in § 1, searches for emission from most of these objects have been conducted before by other air shower arrays (e.g., Alexandreas et al. 1993a; Amenomori et al. 1994) with null results. Also, experiments utilizing the atmospheric Cerenkov technique (e.g., Kerrick et al. 1995b; Karle et al. 1995) have not detected emission from most of these objects, with the notable exception of Markarian 421. The Whipple flux limits (Kerrick et al. 1995b) are, in general, the lowest of those published, but they are over limited time scales and so do not address the question of variability in the AGN emission.

The flux limits quoted by the Cygnus (Alexandreas et al. 1993a) and Tibet (Amenomori et al. 1994) experiments have values lower than our results. Part of the reason for this is that Cygnus and Tibet have lower estimated energy thresholds than CASA-MIA, so their flux limits are affected less by the gamma rays' interaction with the CMBR. However, as stated in § 5, the differences must also be caused partly by the method of flux limit calculation because their limits are more restrictive than ours even if we do not include the CMBR attenuation in our calculation. This is in spite of the fact that our model-independent limits on the ratio of gamma rays to cosmic rays (f_γ^{90}) are much lower than both experiments (compare the results of Table 2 in this work to those of Table 1 in Alexandreas et al. 1993a and Table 1 in Amenomori et al. 1994), as would be expected due mainly to the larger data set and muon coverage. In addition, our data set covers different time periods than those in the above searches and therefore provides further limits on flux variability.

The relevant spectrum for comparison with Markarian 421 is one connecting the EGRET and Whipple measurements. If we use the original EGRET (Lin et al. 1993) and Whipple (Punch et al. 1992), the differential spectral index is 2.07. Uncertainties in this index are difficult to estimate because of the observed variability of Markarian 421 (Schubnell et al. 1996). The continuous flux limits results for Markarian 421 are shown in Figure 3. The solid line is the spectrum obtained by connecting the EGRET and Whipple measurements, and the dashed line shows that spectrum after pair production with the CMBR is included.

The flux limits obtained in this work are not low enough to indicate whether there is any reduction in the Mrk 421 gamma-ray flux relative to what would be expected based on the EGRET and Whipple measurements. This is in contrast to the limits set by the Cygnus (Alexandreas et al. 1993a) and Tibet (Amenomori et al. 1994) experiments which are below the EGRET-Whipple spectrum, but as discussed in the previous sections, the methods for calculating the flux limits are different enough that direct comparison is not appropriate. We only note that our limit on f_γ^{90} for Markarian 421 is 6 times lower than the Cygnus limits (Alexandreas et al. 1993a).

Table 3 shows the maximum daily, weekly, and monthly excess for the muon-poor data set of each AGN. This search also yields no significant signals. For 32 candidate sources each with 1330 observation days, we expect 1.3 objects to have a day with an excess greater than 4 σ just from statistical fluctuations of the background. We see one. We consider all of these distributions to be consistent with random fluctuations of the cosmic-ray background. Figure 4 shows the distribution of daily, weekly, and monthly excesses for the muon poor data set of Markarian 421 along with the expected distribution if the excesses and deficits are due to Gaussian fluctuations of the cosmic-ray background. As with all the other AGNs in this study, the data and Gaussian distributions are consistent with each other. In particular, we see no significant excess for the time period near the 1994 May 14 and 15 burst from Markarian 421 detected by the Whipple Collaboration (Kerrick et al. 1995a).

The authors gratefully acknowledge the assistance of the Command and staff of the US Army Dugway Proving Grounds. We thank M. Cassidy for technical support at Dugway. We also thank S. Golwala, M. Galli, J. He, H. Kim, L. Nelson, M. Oonk, P. Rauske, K. Riley, and Z. Wells for help with the data processing. We thank M. Schubnell for helpful discussions. This work is supported in part by the National Science Foundation and the US Department of Energy. J. W. Cronin and R. A. Ong acknowledge the support of the W. W. Grainger Foundation and R. A. Ong also thanks the Alfred P. Sloan Foundation for their support. The equatorial coordinates of the AGNs in Table 1 were obtained using the NASA/IPAC Extragalactic Database (NED) which is operated by the Jet Propulsion Laboratory, California Institute of Technology, under contract with National Aeronautics and Space Administration.

REFERENCES

Alexandreas, D. E., et al. 1993a, ApJ, 418, 832
Alexandreas, D. E., et al. 1993b, Nucl. Instr. Meth., A328, 570
Amenomori, M., et al. 1994, ApJ, 429, 634
Baillon, P., et al. 1993, Astroparticle Phys., 1, 341
Biermann, P. L., & Strittmatter, P. A. 1987, ApJ, 322, 643
Borione, A., et al. 1993, Proc. of 23d Int. Cosmic-Ray Conf. (Calgary), 1, 357
Borione, A., et al. 1994a, Nucl. Inst. Meth., A346, 329
Borione, A., et al. 1994b, Phys. Rev. D, 49, 1171
Cassiday, G. L., et al. 1989, Phys. Rev. Lett, 62, 383
Catanese, M. A. 1994, Ph.D. thesis, Univ. Michigan
Dermer, C. D., & Schlickeiser, R. 1982, Science, 257, 1642
Dingus, B. L., et al. 1988, Phys. Rev. Lett, 61, 1906
Dube, R. R., Wickes, W. C., & Wilkinson, D. T. 1979, ApJ, 232, 333
Elbert, J. W., et al. 1990, Proc. 21st Int. Cosmic-Ray Conf. (Adelaide), 4, 282
Fichtel, C. E., et al. 1994, ApJS, 94, 551
Gould, J. R., & Schréder, G. P. 1967, Phys. Rev., 155, 1408
Greisen, K. 1960, Ann. Rev. Nucl. Sci., 10, 63
Hartman, R. C., et al. 1994, in AIP Conf. Proc. 304, Second Compton Symposium, ed. C. E. Fichtel, N. Gehrels, & J. P. Norris (New York: AIP), 563
Helene, O. 1983, Nucl. Instr. Meth., 212, 319
Hess, V. 1912, Physik. Z., 13, 1084
Karle, A., et al. 1995, Astroparticle Phys., 4, 1
Kawada, M., et al. 1994, ApJ, 425, L89

Kerrick, A. D., et al. 1995a, ApJ, 438, L59
Kerrick, A. D., et al. 1995b, ApJ, 452, 588
Kniffen, D. A., et al. 1993, ApJ, 411, 133
Li, T. P., & Ma, Y. Q. 1983, ApJ, 272, 317
Lin, Y. C., et al. 1993, ApJ, 401, L61
MacMinn, D. & Primack, J. R. 1995, in TeV Gamma Ray Astrophysics, ed. H. Völk & F. Aharonian (Space Sci. Rev.), in press
Mather, J. C., et al. 1994, ApJ, 420, 439
Mattox, J. R., et al. 1993, ApJ, 410, 609
McKay, T. A., et al. 1993, ApJ, 417, 742
Mohanty, G., et al. 1993, in Proc. of 23d Int. Cosmic Ray Conf. (Calgary), 1, 440
Muller, D., et al. 1991, ApJ, 374, 356
Nagano, M., et al. 1984, J. Phys., G10, 1295
Protheroe, R. J. 1986, MNRAS, 221, 769
Punch, M., et al. 1992, Nature, 358, 477
Rachen, J. P., & Biermann, P. L. 1993, A&A, 272, 161
Rachen, J. P., Stanev, T., & Biermann, P. L. 1993, A&A, 273, 377
Samorski, M., & Stamm, W. 1983, ApJ, 268, L17
Schubnell, M., et al. 1996, ApJ, 460, 644
Sinclair, D. 1989, Nucl. Instrum. Meth., A278, 583
Stanev, T., Gaisser, T. K., & Halzen, F. 1985, Phys. Rev. D, 32, 1224
Stecker, F. W. 1971, Cosmic Gamma Rays (Washington, DC: NASA)
Stecker, F. W., de Jager, O. C., & Salamon, M. H. 1992, ApJ, 390, L49
Szabo, A. P., & Protheroe, R. J. 1992, in AIP Conf. Proc. 264, Particle Acceleration in Cosmic Plasmas, ed. G. P. Zank & T. K. Gaisser (New York: AIP), 304
Tyson, J. A. 1990, in IAU Symp. 139, The Galactic and Extragalactic Background Radiation, ed. S. Bowyer & Ch. Leinert (Dordrecht: Kluwer), 245
von Montigny, C., et al. 1995, ApJ, 440, 525
Weekes, T. C., et al. 1989, ApJ, 342, 379